

## 钯纳米粒子的形貌可控合成与催化性能

茹婷婷<sup>1</sup> 初学峰<sup>1,2</sup> 石莹岩<sup>1</sup> 郑文琦<sup>1</sup> 郭 研<sup>1</sup> 杨小天<sup>\*,2</sup> 蒋 锴<sup>\*,3</sup>

(<sup>1</sup> 吉林建筑大学基础科学部, 长春 130118)

(<sup>2</sup> 吉林建筑大学吉林省建筑电气综合节能重点实验室, 长春 130118)

(<sup>3</sup> 长春中医药大学附属医院, 长春 130021)

**摘要:** 借助于一种全新的表面活性剂 *N,N*-dimethyloctadecylammonium bromide acetate sodium (OTAB-Na), 成功实现了对小尺寸钯纳米粒子微结构的控制。通过对合成条件的微扰, 高度均匀且分散性良好的枝化结构和凹面体结构的钯纳米粒子被成功地制备。催化测试 (利用氨硼烷作为氢化试剂来还原 4-硝基苯酚为 4-胺基苯酚) 发现, 钯纳米粒子的催化活性与其微观纳米结构相关, 其中枝化结构的钯纳米粒子表现出了更为突出的催化性能。

**关键词:** 钯; 贵金属; 纳米粒子; 凹面体; 枝化结构

中图分类号: O614.82\*3

文献标识码: A

文章编号: 1001-4861(2017)10-1835-08

DOI: 10.11862/CJIC.2017.193

## Shape-Controlled Synthesis of Pd Nanocrystals with Remarkable Enhanced Catalytic Performance

RU Ting-Ting<sup>1</sup> CHU Xue-Feng<sup>1,2</sup> SHI Ying-Yan<sup>1</sup> ZHENG Wen-Qi<sup>1</sup>

GUO Yan<sup>1</sup> YANG Xiao-Tian<sup>\*,2</sup> JIANG Kai<sup>\*,3</sup>

(<sup>1</sup>Department of Basic Science, Jilin Jianzhu University, Changchun 130118, China)

(<sup>2</sup>Jilin Provincial Key Laboratory of Architectural Electricity & Comprehensive Energy Saving,

Jilin Jianzhu University, Changchun 130118, China)

(<sup>3</sup>Affiliated Hospital to Changchun University of Chinese Medicine, Changchun 130021, China)

**Abstract:** A morphology-evolution of Pd nanocrystals was successfully triggered by using *N,N*-dimethyloctadecylammonium bromide acetate sodium (OTAB-Na) as the capping agent. Uniform and monodisperse dendritic and concave Pd nanocrystals were synthesized by directly changing the pH value of the reaction solution. In the following catalytic test of liquid-phase reduction of 4-nitrophenol (4-NP) by ammonia-borane complex (AB), the as-obtained Pd nanocrystals exhibit a shape-dependent catalytic properties, in which the dendritic nanosphere is the better one.

**Keywords:** Pd; noble metal; nanoparticle; concave; dendritic

收稿日期: 2017-03-21。收修改稿日期: 2017-07-19。

国家自然科学基金(No.51672103)和国家科技部重大专项(No.2016YFB0401103)资助项目。

\*通信联系人。E-mail: hanyxt@163.com, jiangkaitiamei@sina.com

## 0 Introduction

During the past decades, noble metal nanostructures have attracted considerable research interest because of their unique chemical and physical properties are widely applied in electronic, catalytic, photonic, biologic and energy-related areas<sup>[1-4]</sup>. However, their ultra-low abundances in nature and the ultra-high prices have seriously limited their further applications. Thus, optimizing the properties of noble metals to reduce the overall cost has become one of the most important and urgent problems to be solved in nano-science. In generally speaking, the morphologies of noble metals can strongly affect their properties, especially for a catalytic reaction<sup>[5-8]</sup>. That is because the stability of intermediate is highly depending on the interplanar spacing of the noble metals, which is determined by the morphology strongly. Designing and fabricating the noble metals with desirable nanostructures can endow them with superior catalytic activity, stability and selectivity.

Among the various kinds of noble metal nanostructures, there are two specially ones, highly dendritic and concave morphologies, which have been paid more attention in the recent years. For a dendritic nanostructure, it has ultra-small building block and open channel. Thus such kind of noble metals always have high surface area and be rich in edge/corner atoms, which makes them play the important role of highly active sites in catalytic reactions<sup>[9]</sup>. On the other hand, although the concave morphology also possess a large number of atoms at edges, the more important structural feature is the exposed high-index surface. As a result of the high density of low-coordinated atoms in the forms of atomic steps and kinks, high-index facets are generally more active toward specific reactions than low-index planes that are composed of closely packed surface atoms<sup>[10]</sup>. Many kinds of dendritic and concave noble metal nanostructures are successfully fabricated. For instance of dendritic nanostructure, directly growth can achieve the main purpose. Wang and co-works have shown us a series of excellent works by using block copolymers to induce the formation of highly dendritic Pt or Pt on Pd nanostructures<sup>[11-13]</sup>. Huang's group has reported a facile

synthesis by using hexadecylpyridinium chloride as capping agents to produce Pd nanospheres with highly ordered porous features and perpendicular pore channels<sup>[9]</sup>. Very recently, Pt nanohelices with highly ordered horizontal pore channels are also created by Wang and co-works. A new kinds of surfactant, *N,N*-dimethyloctadecylammonium bromide acetate sodium (OTAB-Na) exhibited powerful capability to control the growth of Pt metals<sup>[14]</sup>. On the other hand, for concave nanostructures, seeded growth method and galvanic replacement reaction-assisted process are more efficient. Xiong's group has found that  $\text{Ru}^{3+}$  can induce the morphology-evolution of Pd nanostructures from cube to concave cube<sup>[15]</sup>. The similar phenomenon has been also observed by Zheng's group, that they found  $\text{Cu}^{2+}$  can assist the formation of concave Pt nanostructures<sup>[10]</sup>. Moreover, concave Au and Au@Pd nanostructures are successfully obtained by a seeded method<sup>[16-18]</sup>. By carefully referring to the above mentioned manuscripts, it is considered that investigating the shape-evolution process of noble metals is very important to optimize their catalytic properties. However, to the best of our knowledge, the shape-evolution process of noble metals from concave to dendritic nanocrystals is still no observed in one synthetic system. Thus, the challenge in the synthesis still exists.

Herein Pd element has been chosen as the research objective owing to its high performance in many industrial applications. Nanostructured Pd serves as the primary catalyst for various organic reactions and also has remarkable performance in hydrogen storage and hydrogen sensing<sup>[19-21]</sup>. Thus, investigating the morphology-effect of Pd nanocatalyst is very important. Inspired by the above mentioned representative works, OTAB-Na has been used here. Fortunately, a morphology-evolution has been observed. In a typical synthesis, a transparent aqueous solution contained OTAB-Na and certain amount of NaOH or HCl is heated at 60 °C for a while, following by addition of  $\text{Na}_2\text{PdCl}_4$  solution and freshly prepared aqueous ascorbic acid solution in turn. The reaction is holding for 3 hours and finally the resulting colloidal product is collected by centrifugation and washed three times with ethanol.

## 1 Experimental

### 1.1 Preparation of *N,N*-dimethyloctadecylammonium bromide acetate sodium salt ( $C_{18}H_{37}N(CH_3)_2(CH_2COONa) \cdot Br$ , OTAB-Na)

This synthesis is according to the recently reported method<sup>[14]</sup>. Typically, 10 mmol *N,N*-dimethyloctadecylamine was reacted with 5 mmol sodium bromoacetate in 50 mL ethanol at 80 °C for 24 h. Herein, it should be noticed that excess amount of *N,N*-dimethyloctadecylamine was added in the reaction system to promote the quaternization reaction. After cooling down to room temperature, the solution was concentrated on a rotary evaporator to about 4 mL, following by addition of excess anhydrous diethyl ether to help the precipitation of OTAB-Na product. And in this step, the un-reacted *N,N*-dimethyloctadecylamine can be removed easily and completely.

### 1.2 Preparation of Pd nanocubes

OTAB-Na (90 mg) was dissolved in 10 mL water to form a transparent solution by heating the mixture at 60 °C for a while. Then 2 mL HCl aqueous solution ( $0.1 \text{ mol} \cdot \text{L}^{-1}$ ) was added followed by injection of 1 mL  $\text{Na}_2\text{PdCl}_4$  solution ( $20 \text{ mmol} \cdot \text{L}^{-1}$ ) and 1 mL ascorbic acid solution ( $0.1 \text{ mol} \cdot \text{L}^{-1}$ ) in turn. Three hours later, the products were collected by centrifugation with the help of ethanol (ethanol makes the important role of anti-solvent towards OTAB-Na molecules) and washed three times with water and ethanol.

### 1.3 Preparation of Pd concave nanocubes

OTAB-Na (90 mg) was dissolved in 10 mL water to form a transparent solution by heating the mixture at 60 °C for a while. Then 1 mL  $\text{Na}_2\text{PdCl}_4$  solution ( $20 \text{ mmol} \cdot \text{L}^{-1}$ ) and 1 mL ascorbic acid solution ( $0.1 \text{ mol} \cdot \text{L}^{-1}$ ) were in turn. Three hours later, the products were added collected by centrifugation with the help of ethanol and washed three times with water and ethanol.

### 1.4 Preparation of Pd sea anemone-like nanospheres

OTAB-Na (90 mg) was dissolved in 10 mL water to form a transparent solution by heating the mixture at 60 °C for a while. Then 2 mL NaOH aqueous solution ( $0.1 \text{ mol} \cdot \text{L}^{-1}$ ) was added followed by injection of 1 mL  $\text{Na}_2\text{PdCl}_4$  solution ( $20 \text{ mmol} \cdot \text{L}^{-1}$ ) and 1 mL ascorbic acid solution ( $0.1 \text{ mol} \cdot \text{L}^{-1}$ ) in turn. Three hours later, the

products were collected by centrifugation with the help of ethanol and washed three times with water and ethanol.

### 1.5 Preparation of Pd octahedrons

OTAB-Na (90 mg) was dissolved in 10 mL water to form a transparent solution by heating the mixture at 60 °C for a while. Then 3 mL NaOH aqueous solution ( $0.1 \text{ mol} \cdot \text{L}^{-1}$ ) was added followed by injection of 1 mL  $\text{Na}_2\text{PdCl}_4$  solution ( $20 \text{ mmol} \cdot \text{L}^{-1}$ ) and 1 mL ascorbic acid solution ( $0.1 \text{ mol} \cdot \text{L}^{-1}$ ) in turn. Three hours later, the products were collected by centrifugation with the help of ethanol and washed three times with water and ethanol.

### 1.6 Characterization

The X-ray diffraction patterns of the products were collected on a Rigaku-D/max 2500 V X-ray diffractometer with Cu  $K\alpha$  radiation ( $\lambda=0.15418 \text{ nm}$ ), with an operation voltage and current maintained at 40 kV and 40 mA ( $2\theta=30^\circ\sim70^\circ$ ). Transmission electron microscopic (TEM) images were obtained with a TECNAI G2 high-resolution transmission electron microscope operating at 200 kV.

### 1.7 Liquid-phase reduction of 4-nitrophenol (4-NP) by ammonia-borane complex (AB)

The catalytic test was directly taken in a quartz cuvette and monitored by the UV-Vis spectrophotometer (UV-3600). 4-NP ions ( $0.01 \text{ mol} \cdot \text{L}^{-1}$ ) aqueous solution was prepared by mixing 4-NP and NaOH in water with the molar ratio of 1:1. For a typical catalytic process, 0.02 mL nitrophenol and 0.05 mL AB aqueous solution were mixed in 3 mL  $\text{H}_2\text{O}$ . Then 100  $\mu\text{L}$  Pd colloid solution ( $0.002 \text{ mol} \cdot \text{L}^{-1}$ , details are shown in Table S1) was quickly added. The intensity of the absorption peak at 400 nm for 4-NP ions was monitored along with time.

## 2 Results and discussion

The structure information about the as-formed Pd nanostructures are first characterized by transmission electron microscopy (TEM), high-resolution transmission electron microscopy (HRTEM), and powder X-ray diffraction (XRD). As shown in Fig.S1 (a low-magnification TEM image), monodisperse nanoparticles with diameters of approximately 20 nm are obtained. No scattered and smaller-sized Pd nanoparticles could be found, suggesting the high purity and relatively high quality. Interestingly, from the enlarged TEM image in Fig.1a and b, we can see that the products exhibit a

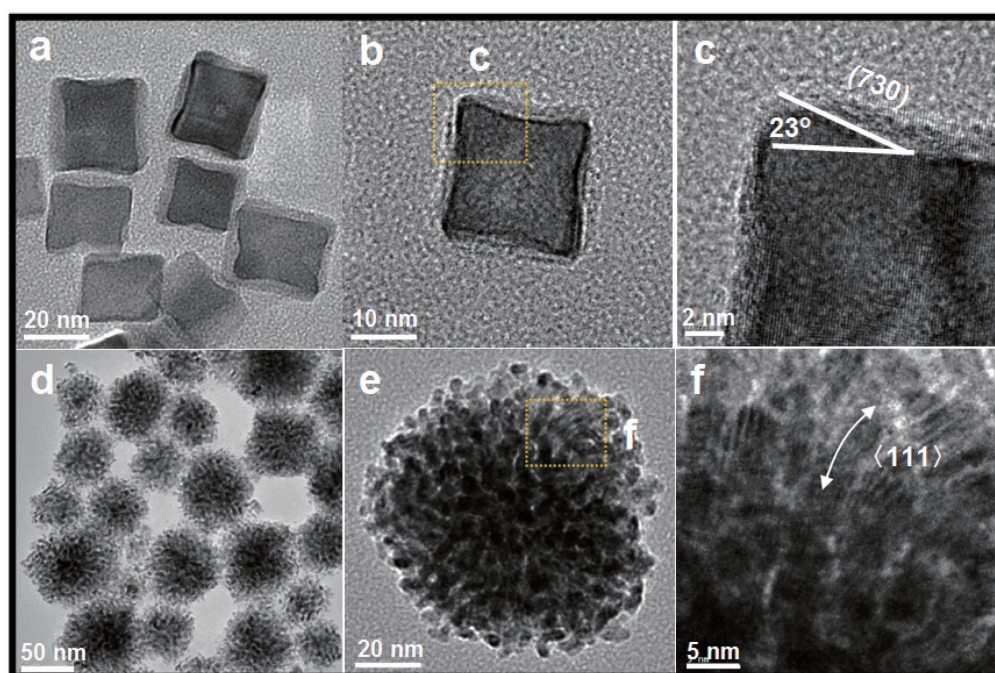


Fig.1 TEM images of (a) to (c): concave Pd cubes; (d) to (f): dendritic Pd nanospheres

typical concave nanostructure: each face of the cube is concave at the center. Referring to the previous reports<sup>[15]</sup>, the concave cubes are enclosed by (730) facets (as shown in Fig.1c). Further X-ray diffraction was conducted on product nanocubes spread on a glass substrate. The pattern is well corresponding to fcc Pd metal (Fig.2, PDF No.87-0641).

Very interesting, it is found that the morphology of Pd nanocrystal is highly dependent on the pH value of the growth solution. With the corresponding TEM image shown in Fig.1d, uniform and monodisperse Pd nanospheres with highly porous structural feature are obtained when 2 mL NaOH ( $0.1 \text{ mol} \cdot \text{L}^{-1}$ ) aqueous solution is added in the solution before the injection of Pd metal salt. Compared with the concave cubes, the particle size is grown up to sub 50 nm in average. Importantly, it is found that the building blocks of the nanospheres are highly dendritic short nanowires, which could be distinguished easily from the enlarge TEM image in Fig.1e. The HR-TEM image in Fig.1f confirms that the short nanowires are grew along with Pd  $\langle 111 \rangle$  direction. Further increasing the feeding amount of NaOH aqueous solution could destroy the original 3D nanostructures, but the final products are uniform sub 5 nm octahedrons (Fig.S2). Another control experiment has

also been taken by decreasing the pH value of the growth solution by addition of HCl aqueous solution. Fig.S3 is the typical TEM result which obtained by the addition of 2 mL HCl ( $0.1 \text{ mol} \cdot \text{L}^{-1}$ ). Sub 11 nm Pd cubes are observed. There is no concave particles could be found from the TEM images. We also investigate the temperature-effect towards the shape-evolution of Pd nanocrystal. With the data shown in Fig.S4, under the similar synthetic condition (increasing the reaction temperature to 80 °C), sea anemone-like nanospheres are disappeared and the products exhibit irregular shapes.

It is well known that the morphology of Pd

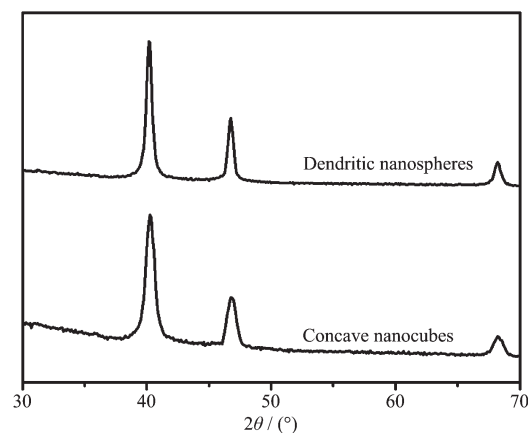


Fig.2 XRD patterns of dendritic nanospheres and concave nanocubes



nanocrystal is determined by the deposited rate of Pd atoms in different directions. The morphology-evolution is described in Fig.3. For acid solution, protonation reaction of OTAB-Na will happen, as a result OTAB-Na should be in the form of OTAB-H ( $\text{OTAB-Na} + \text{H}^+ \rightarrow \text{OTAB-H} + \text{Na}^+$ ). Thus, the coordination ability of the capping agent to  $\text{Pd}^{2+}$  becomes so weak. At the same time,  $\text{Br}^-$  ions play the critical role to induce the whole synthesis because that they can stabilize the {100} faces of Pd nanocrystals efficiently<sup>[22-25]</sup>. The structural formula of OTAB-Na (as shown in Fig.S5) indicates its weak alkalinity ( $\text{OTAB-Na} + \text{H}_2\text{O} \rightleftharpoons \text{OTAB-H} + \text{OH}^-$ ), thus the OTAB-Na molecule can react with water to generate free  $\text{OH}^-$  ions under heating treatment (without addition of HCl). The increased pH value enhances the reducing ability of ascorbic acid (AA). Compared with the acid condition, the reaction rate could be highly accelerated when no HCl is added in the growth solution<sup>[26-27]</sup>. As reported previously, when the side faces are capped by  $\text{Br}^-$ , the reduced atoms prefer to nucleate and grow from the edges and corners. When the reducing rate of metal atoms is greater than the surface diffusion rate on the particle, the newly deposited atoms will not migrate timely to the side surfaces, causing the formation of concave nanocubes<sup>[27-28]</sup>. Thus, the formation mechanism of the concave nanocubes is easy to be understood that the large amount of as-generated Pd atoms are deposited along with the  $\langle 111 \rangle$  direction instead of {100} faces. Furthermore, such growth orientation could be enlarged by further increasing the pH value of the reaction solution by direct addition of NaOH aqueous solution in. When 3 mL NaOH aqueous solution ( $0.1 \text{ mol} \cdot \text{L}^{-1}$ ) is

added, no Pd atoms deposited on {100} surface, but grew along with  $\langle 111 \rangle$  direction to form the twist and short nanowires. At the same time, it is believed that in such strong alkaline solution, OTAB-Na is dissociated completely. The presence of  $-\text{COO}^-$  groups makes the long alkyl chains bonded on the surface of Pd atoms strongly. By the help of van der Waals force, numbers of short Pd nanowires are assembled together to form a sea anemone-like porous nanospheres with highly dendritic structural feature. It is the first time that using one kind of surfactants induces the formation of both the dendritic and concave nanostructures successfully, which could help us to investigate the morphology-effect of Pd nanocrystals for the catalytic performances in-depth. As a short summary, OTAB-Na plays the key role in our synthesis. Compared with the traditional quaternary ammonium salt, such as CTAB and CTAC, the presence of carboxyl group in OTAB-Na makes it more different. Firstly, OTAB-Na can hydrolyze partly and generate free  $\text{OH}^-$  in the reaction solution, which could speed up the reducing rate and change the atom-deposited form. Secondly, carboxyl group increases the bonding force between surfactants and generated noble metal atoms. In such condition, some special behaviors of the organic molecules can shift to the noble metals. These are considered as the main reasons for the morphology-evolution of Pd nanocrystals.

The catalytic liquid-phase reduction of *p*-nitrophenol (4-NP) by ammonia borane (AB) is chosen here to help us to evaluate the catalytic performances of dendritic and concave Pd nanoparticles. Compared with the traditional hydrogenation reagent,  $\text{NaBH}_4$ , AB compound is safer and has higher hydrogen capacity<sup>[29-30]</sup>. Using AB to instead of  $\text{NaBH}_4$  has become the research hot spot in recent years. Before the starting of the catalytic reaction, NaOH has been added in 4-NP aqueous solution to make the formation of 4-NP ions, which has strong absorption peak at 400 nm. The whole catalytic process is monitored by UV-Vis spectrophotometer. Fig. 4a shows the typical conversion ratio of 4-NP as function of reaction time over two catalysts under the same conditions. Concave cubes have shown much poorer catalytic performance. 18 min later, only about 33% 4-NP has been converted. On the opposite, the catalytic

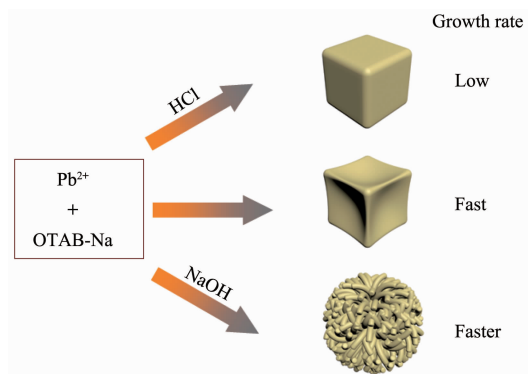
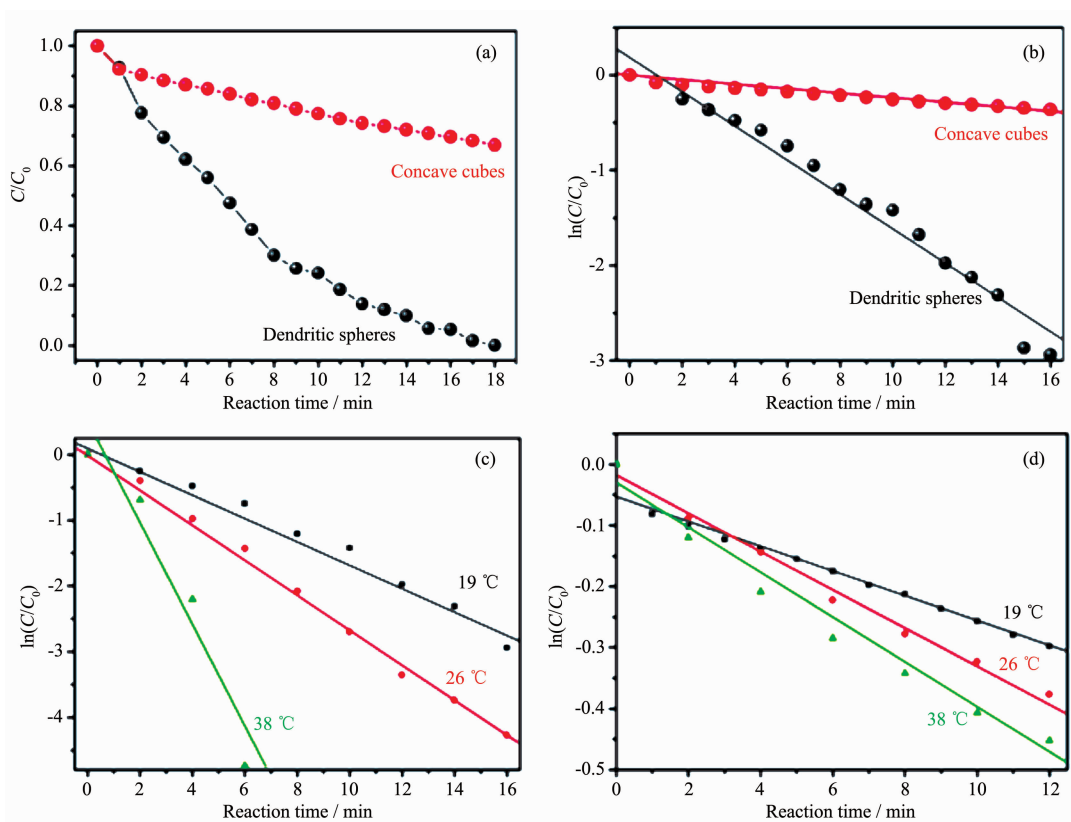


Fig.3 Schematic illustration of the shape evolution of Pd nanocrystals



(a) plots of time vs  $C/C_0$  by different catalysts at 19 °C; (b) plots of time vs  $\ln(C/C_0)$  by different catalysts at 19 °C; (c) and (d) plot of time vs  $\ln(C/C_0)$  at different temperatures by dendritic and concave Pd nanocrystals, respectively

Fig.4 Catalytic test of dendritic and concave Pd nanocrystals in liquid-phase reduction of 4-NP by AB

activity of dendritic Pd nanospheres is much higher. With the addition of the catalyst in the reaction system, the original yellow solution faded fast and finally became colorless with 18 min. The corresponding plot of time by dendritic Pd nanospheres is shown in Fig.4a black line. The greater slope of the curve indicating the higher catalytic activity compared with the concave one. Fig.4b shows the  $\ln(C/C_0)$  ( $C$  and  $C_0$  represent the concentration of 4-NP at time ( $t$ ) and at the beginning of the reaction, respectively) versus time of the two samples at  $T=19\text{ }^{\circ}\text{C}$ . A rapid and almost linear evolution is observed between  $t$  and  $\ln(C/C_0)$ , which suggesting both of the two plots followed first-order reaction kinetics very well. Thus the rate constant  $k$  can be calculated from the rate equation  $\ln(C/C_0)=-kt$ . The value is 0.17 and  $0.02\text{ min}^{-1}$  for dendritic and concave Pd nanocrystals at 19 °C, respectively. Be similar with the previous reports, increasing the feeding amount of catalyst can largely accelerate the catalyst rate. With the data shown in Fig.S6, the reaction can be finished with 12 min by

addition of double amount of catalyst.

Fig.4c and e have shown the plot of  $\ln(C/C_0)$  versus time at various reaction temperatures of dendritic and concave Pd nanocrystals, respectively. The nearly horizontal lines indicate that increasing the reaction temperature can just increase the reaction rate but can't change the catalytic kinetic model. The values of  $k$  at various temperatures are calculated from the slope of the linear part of each plot in Fig.4c and e to determine the activation energy. Fig.4d and f show the linear fitting of  $\ln k$  and  $1/T$ . The apparent activation energy ( $E_a$ ) can be calculated from the Arrhenius equation:  $\ln k = \ln A - E_a/(RT)^{[31]}$ . The calculated  $E_a$  value is approximately 35.0 and  $20.7\text{ kJ}\cdot\text{mol}^{-1}$  for concave and dendritic Pd nanocrystals, respectively, where  $\ln A$  is the intercept of the line and  $R$  is the gas constant. The above results have firmly confirmed that the as-obtained dendritic spheres have higher catalytic properties than the concave cubes.

Finally, a cycling test has also been done to investigate the catalytic stability of the dendritic nano-

spheres. As shown in Fig.5, the reaction time of the second cycle is faster than the first cycle. The possible reason is considered that the hydrogenation reaction in first cycle has clean the surface-bonded OTAB-Na molecules. Thus, the catalytic rate is accelerated. For the following three cycles, the as-obtained dendritic catalyst kept well their activity. The whole reaction could be finished within 15 min.

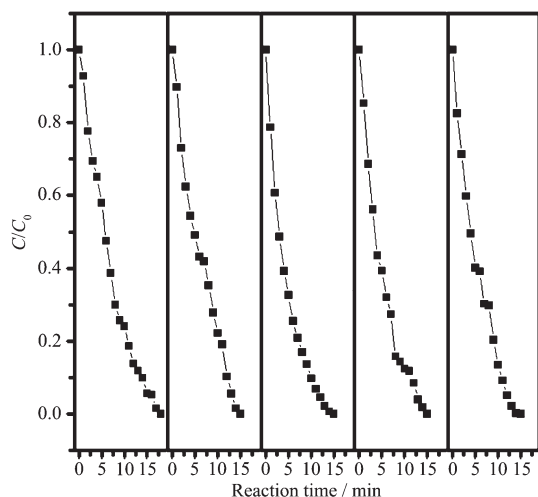


Fig.5 Cycling test catalyzed by dendritic nanospheres

### 3 Conclusions

In all, a morphology-evolution process of Pd nanocrystals has been observed by using OTAB-Na as the capping agent. Simply changing the pH value of the growth solution can produce high quality Pd nanocubes, concave nanocubes, dendritic spheres and small sized octahedrons. The main effect of OTAB-Na for the particle growth could be divided to three parts:  $\text{Br}^-$  can stabilize Pd {100} faces; OTAB-Na can react with water to generate  $\text{OH}^-$  and carboxyl group can make the long alkyl chains bonded on the surface of Pd atoms strongly, which could trigger the self-assembling performance. It is the first time to achieve the goal of using one kind surfactant to induce the formation of both the dendritic and concave Pd nanostructures. In the following catalytic test of liquid-phase reduction of 4-NP by AB, the as-obtained dendritic spheres have shown higher catalytic properties, which is a typical shape-dependent catalytic properties.

Supporting information is available at <http://www.wjhxxb.cn>

### References:

- [1] Sun Y G, Xia Y N. *Science*, **2002**,**298**:2176-2179
- [2] Chiu C, Wu H, Yao Z, et al. *J. Am. Chem. Soc.*, **2013**,**135**: 15489-15500
- [3] Lim B, Jiang M, Camargo P, et al. *Science*, **2009**,**324**:1302-1305
- [4] Xia Y, Xiong Y, Lim B, et al. *Angew. Chem. Int. Ed.*, **2009**, **48**:60-103
- [5] Xia B, Ng W, Wu H, et al. *Angew. Chem. Int. Ed.*, **2012**,**51**: 7213-7216
- [6] Xia B, Wu H, Yan Y, et al. *J. Am. Chem. Soc.*, **2013**,**135**: 9480-9485
- [7] Jin M, Zhang H, Xie Z, et al. *Energy Environ. Sci.*, **2012**,**5**: 6352-6357
- [8] Wu Y, Cai S, Wang D, et al. *J. Am. Chem. Soc.*, **2012**,**134**: 8975-8981
- [9] Huang X, Li Y, Chen Y, et al. *Angew. Chem. Int. Ed.*, **2013**, **52**:2520-2524
- [10] Huang X, Zhao Z, Fan J, et al. *J. Am. Chem. Soc.*, **2011**, **133**:4718-4721
- [11] Wang L, Nemoto Y, Yamauchi Y. *J. Am. Chem. Soc.*, **2011**, **133**:9674-9677
- [12] Wang L, Yamauchi Y. *J. Am. Chem. Soc.*, **2009**,**131**:9152-9253
- [13] Wang L, Yamauchi Y. *J. Am. Chem. Soc.*, **2013**,**135**:16762-16765
- [14] Song S, Wang X, Li S, et al. *Chem. Sci.*, **2015**,**6**:6420-6424
- [15] Long R, Rao Z, Mao K, et al. *Angew. Chem. Int. Ed.*, **2015**, **54**:2425-2430
- [16] Lu C, Prasad K, Wu H, et al. *J. Am. Chem. Soc.*, **2010**,**132**: 14546-14553
- [17] Yu Y, Zhang Q, Liu B, et al. *J. Am. Chem. Soc.*, **2010**,**132**: 18258-18265
- [18] Hong J, Lee S, Lee, Han Y. *J. Am. Chem. Soc.*, **2012**,**134**: 4565-4568
- [19] Bosch S, Schutyser W, Koelewijn S, et al. *Chem. Commun.*, **2015**,**51**:13158-13161
- [20] Xia Y, Liu Z, Ge R, et al. *Chem. Commun.*, **2015**,**51**:11233-11235
- [21] Li J, Zhu Q, Xu Q. *Chem. Commun.*, **2015**,**51**:10827-10830
- [22] Xia Y, Xia X, Peng H. *J. Am. Chem. Soc.*, **2015**,**137**:7947-7966
- [23] Peng H, Xie S, Park J, et al. *J. Am. Chem. Soc.*, **2013**,**135**: 3780-3783
- [24] Peng H, Park J, Zhang L. *J. Am. Chem. Soc.*, **2015**,**137**: 6643-6652

- [25]Xia X, Choi S, Herron J, et al. *J. Am. Chem. Soc.*, **2013**, **135**:15706-15709
- [26]Niu W, Zhang W, et al. *Chem. Mater.*, **2014**,**26**:2180-2186
- [27]Shao Z, Zhu W, Wang H, et al. *J. Phys. Chem. C*, **2013**,**117**: 14289-14294
- [28]Zhang H, Jin M, Xia Y. *Angew. Chem., Int. Ed.*, **2012**,**51**: 7656-7673
- [29]Wang X, Liu D, Song S, et al. *J. Am. Chem. Soc.*, **2013**, **135**:15864-15872
- [30]Chandra M, Xu Q. *J. Power Sources*, **2006**,**159**:855-860
- [31]Zeng J, Zhang Q, Chen J Y, et al. *Nano Lett.*, **2010**,**10**:30-35